Hindawi
Advances in Civil Engineering
Volume 2021, Article ID 5534002, 14 pages
https://doi.org/10.1155/2021/5534002

Research Article

Influence of Concrete Sludge Addition in the Properties of Alkali-Activated and Non-Alkali-Activated Fly Ash-Based Mortars

Fotini Kesikidou, Stavroula Konopisi, and Eleftherios K. Anastasiou

Laboratory of Building Materials, School of Civil Engineering, Aristotle University of Thessaloniki, Thessaloniki 54124, Greece

Correspondence should be addressed to Eleftherios K. Anastasiou; elan@civil.auth.gr

Received 10 February 2021; Revised 15 April 2021; Accepted 27 April 2021; Published 7 May 2021

Academic Editor: Yingzi Yang

This study investigated the use of concrete sludge, a by-product of the ready-mix concrete industry, in combination with high-calcium fly ash in binary cementless binders. Concrete sludge was used in substitution rates ranging from 0% to 60% in test fly ash-based mortars to determine potential synergy. The mortars were tested for fresh and hardened properties; workability, viscosity, strength development, open porosity, early-age shrinkage, and analytical tests were carried out. A mortar with 50% fly ash and 50% limestone filler as binders was used for comparison purposes. Furthermore, a series of mortars with fly ash and concrete sludge were alkali-activated in order to determine potential strength gain. In the activated mortars, two fractions of concrete sludge were used, under 75 μm and 200 μm, due to different silicon oxide contents, while one mortar was cured at 40°C to investigate the effect of heating on alkali activation. Results show that sludge contributes to the formation of C-S-H and strength development when used in combination with high-calcium fly ash even at high replacement rates. The alkali activation of fly ash-concrete sludge system contributed to early-age strength development and to early-age shrinkage reduction.

1. Introduction

Today, in Europe, it is estimated that fresh concrete waste, at the production stage or the cleaning/washing stage of concrete trucks, is approximately 1–4% by weight of the total concrete produced [1]. After the washing of the barrels with huge amounts of water, up to 1300 liters per truck, the material is left to settle in large sedimentation tanks. From these tanks, the water can be reused to wash the vehicles or as mixing water for new concrete, while the sediment is concentrated at the bottom in the form of sludge [2]. This wet concrete sludge is difficult to handle and also has an alkaline pH value which makes the deposit of the material a burden for the environment and human health. In some countries, like UK, Spain, and USA, sludge is classified as a corrosive hazardous material due to its high alkalinity (pH > 11.5) [3–5].

Audo et al. [2] investigated the use of sludge from ready-mixed concrete plants as a substitute for limestone fillers. It has been noted that the rheology of the fresh state mortar is altered with the addition of sludge, leading to the mixture becoming less plastic. Compressive strength varied from a reduction of 30% to an increase of 17%, which is attributed to the different fractions of the sludge (finer than 100 μm and coarser than 100 μm) and the substitution rate of the sand fraction of the mortars [2]. Xi et al. [6] have studied the use of marble and concrete sludge as supplementary cementitious material by replacing cement in mortars. The researchers have found that both materials could be used as fillers, while the use of concrete sludge showed higher compressive strength than marble sludge, probably due to its higher alkalinity.

On the other hand, fly ash is a by-product, deriving from the combustion of coal or lignite, which has been studied extensively over the last years and is already used as supplementary cementitious material [7–9]. Its chemical composition depends on the type of raw material and the methods of the combustion. Fly ashes from the burning of coal typically have low calcium oxides content and classify as siliceous fly ashes with pozzolanic

properties. On the contrary, fly ashes from the burning of lignite are rich in calcium oxides and classify as high-calcium fly ashes with both pozzolanic and self-cementing properties. European Standard EN 450-1 classifies fly ash into two categories: siliceous fly ash, which contains calcium oxides in less than 10%, and calcareous fly ash, which has a content of calcium oxides over 10% [10]. Regardless of the type, the use of fly ash in cement and concrete has both economic and environmental benefits as it enhances the service life of concrete—for example, addition of up to 30% of fly ash in concrete reduces chloride penetration [11]—and reduces the energy consumption and carbon dioxide emissions from the production of cement [12]. Calcareous fly ash is known to exhibit considerable self-cementing properties due to its reactive lime and silica contents [13]. EN 197-1 [14] requires that it must show at least 10 MPa compressive strength at 28 days when mixed with water according to EN 196-1 [15] to be used in blended cements. Researchers have shown that the hydration of calcareous fly ash can be enhanced when used in combination with other supplementary cementitious materials or when alkali-activated [16]. The process of alkali-activation is a field of study that focuses on the use of by-products like fly ash and slag. It includes a chemical reaction by polymerization of aluminosilicate oxides under the influence of silicon solutions in highly alkaline conditions by heating [17]. Over the years, many researchers have focused on the activation of binders such as several types of slag and fly ash [18], metakaolin [19], natural pozzolans [20], and red mud [21]. Extensive research has been conducted in the case of fly ash, studying the properties of siliceous and high-calcium types of fly ash [22–28].

Since cement clinker is accountable for considerable carbon dioxide emission, focus is needed to improve reduced clinker or even clinker-free binders. Although fly ash and concrete sludge have been studied separately as additives in concrete [29–31], no focus has been given so far in the combination of the two binders, in order to develop cement-free binders. Along these lines, the paper attempts to explore the potential improvement of calcareous fly ash hydration by combining it with concrete sludge. Binary mortars based on fly ash and concrete sludge were tested for strength development for an increasing rate of fly ash replacement with concrete sludge. Fresh properties such as plastic viscosity and workability of the mortars were measured and flexural and compressive strength were tested at the ages of 7, 28, and 90 days. Open porosity and volume stability were also determined. *X*-Ray Diffraction (XRD) analysis, simultaneous system of Differential Thermal-Thermogravimetric Analysis (DTA-TG), and Fourier Transform Infrared Spectroscopy (FT-IR), with the technique of Attenuated Total Reflectance (ATR), were used to characterize changes and behavior of the structure. In an effort to explore the effect of concrete sludge on fly ash hydration, a fly ash-limestone filler binary mortar was prepared for comparison purposes. Furthermore, selected fly ash-concrete sludge binary mortars were prepared with a combination of sodium hydroxide and waterglass solutions as activator and tested for strength development.

2. Materials and Methods

2.1. Raw Materials. Concrete sludge was received in wet condition and was subsequently dried, ground in a laboratory ball mill, and sieved. Initially the sieving was carried out through the 75 μm sieve, but it was concluded from the chemical analyses that a lot of the silica present in the sludge (possibly in the form of hardened C-S-H) was retained in the sieve, so the sludge was also sieved through the 200 μm mesh, resulting in testing the material in two levels of fineness (S75 and S200). Calcareous fly ash (FA) originated from a power plant in Greece and was used unprocessed, while limestone filler (LF) was received from a local quarry, already ground to adequate fineness. The particle size distribution (PSD) analyses, of the fly ash, the two concrete sludge types, and the limestone filler were measured by Malvern P.S.A Mastersizer 2000-laser scattering technique and are presented in Figures 1–4, while the mean particle diameters d10, d50, and d90 (denoting that 10%, 50%, and 90%, resp., of each sample are below the reported values) are presented in Table 1.

The total oxides of the binders were determined by Atomic Absorption Spectroscopy analysis–AAS (AAnalyst 400 Perkin Elmer) and are shown in Table 2. The gravimetric determination of total sulphates content (as SO_3) was performed by precipitation under the influence of barium chloride ($BaCl_2$) solution. The loss of ignition (LOI) was determined by combustion of the binders at 1000°C. Additionally, the pore solution pH values of fresh pastes were measured by a pH-Meter 766 Calimatic-Knick.

Natural river sand (0–4) mm was used in all test mortars. A solution of sodium hydroxide (NaOH 6 M) and waterglass in a (1 : 1) ratio in combination with water was used as an activator in the alkali-activated mortars. A polycarboxylic-based superplasticizer was added when required to achieve adequate workability.

2.2. Mix Design. Initially six mortar mixtures (Table 3) were produced with increasing rate of fly ash replacement with concrete sludge, from 0% to 60% wt.%. The finer fraction of concrete sludge (S75) had a chemical composition very close to that of LF and could be considered as filler, while the particle size distribution showed that concrete sludge was considerably finer than LF and also considerably finer than fly ash. From the literature, it is known that the increased fineness of supplementary cementitious materials can promote binder hydration and strength development by improving particle packing and also through the filler effect [32]. Thus, it was decided to use the finer fraction of sludge (S75) in the first batch of mortars, while a binary mortar with 50% fly ash and 50% limestone filler was prepared to compare the reactivity of the sludge with the limestone filler.

Alkali activation was considered at a second mortar batch as a means to enhance the reactivity of the fly ash-concrete sludge system. The fly ash used was calcareous, with free calcium oxide (CaO_{free}) equal to 5.61%, determined according to EN 451-1 [33], and with considerable amounts of silicon dioxide and aluminum oxide. Based on previous research [34], it is possible to use alkali activation to promote

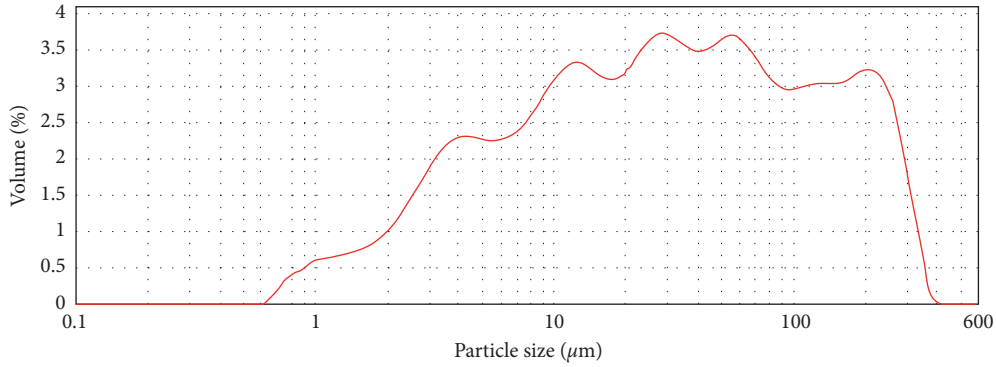

Figure 1: Particle size distribution of calcareous fly ash (FA).

the hydration of such fly ashes, and, therefore, it was decided to repeat three of the initial mortars (the ones with 0%, 20%, and 50% replacement with S75) using a combination of sodium hydroxide: waterglass solutions as activator. The three selected mixtures were decided based on the early strength results of the nonactivated mixtures. Regarding the concrete sludge, it is obvious that sieving of the material has an impact on the content of the silicon dioxide, which in the sludge under 75 μm is 2.28%, whereas in sludge under 200 μm it is 15.01% (Table 2). Since silicon dioxide content is important for the alkali activation process [17], it was decided to test a mortar using 30% replacement with the coarser, richer in silicon dioxide (SiO_2), S200 (AN30). The last mortar was repeated using heating at 40°C for 24 h after casting (AT30) in order to determine possible enhancement of the alkali activation through heating, reaching a second batch of five mortars (Table 4).

Mixing procedure followed 2 min in slow speed and 7 min in fast speed in the mixer, which was selected as appropriate for achieving adequate consistency. Workability was measured with the flow table test according to EN1015-3 [35] and plastic viscosity of the mixtures was also determined with an ICAR rheometer. Then the fresh mortars were cast in prismatic specimens $(40 \times 40 \times 160)\,mm^3$ and were cured for 24 hours in metallic molds at 25°C. Mixture AT30 was cured in an oven at 40°C to investigate the effect of early-age heating on alkali activation. After 24 hours all specimens were demolded and kept at a chamber with 90% RH and 21°C until testing.

2.3. Testing of Hardened Mortars. Compressive strength was measured at the ages of 7, 28, and 90 days according to EN 1015-11 [36]. Open porosity values at 28 days were measured following the RILEM CPC 11.3 Methodology [37] and early-age volume deformation was recorded up to 28 days, while the specimens were kept in a chamber with 50%RH and 21°C. XRD analysis, via a Bruker D2 Phaser diffractometer (CuKa1 radiation, 30 KV/10A, measurement range 5–70° 2θ, step 0,02°) was used for mineralogical characterization of phases. The content of the hydration products and the remaining compounds of calcium hydroxide and calcium carbonate were determined by DTA-TG (SDT 2960, TA Instruments) using N2 atmosphere from 10°C to 1000°C. The mid-IR spectrums (frequency range 4000–400 cm^{-1} at a resolution of 4 cm^{-1}) of samples were collected using a spectrometer (Cary 630 FTIR-Agilent Technologies) with an ATR mode, in order to record significant structural changes of the hydration products.

3. Results and Discussion

3.1. Nonactivated Mortars. Rheology of mortar is affected by multiple factors such the processing energy, the solid concentration, the paste/aggregate and mortar to aggregate/ ratio, air content, and the paste composition [38]. More specifically, in terms of the paste rheology, the fineness of the binder, mineral additions, and chemical admixtures are of vital importance [39]. The chemical composition of the binder is another significant factor and, especially, its content in calcium and aluminum oxides and sulfates. Environmental conditions, such as temperature and humidity levels during mixing, also affect the measured results.

Previous work of the authors has showed that the composition of the fly ash, which is rich in calcium oxides, aluminum oxides, and sulfates, requires a different mixing procedure in order to decrease the viscosity of the mortar and achieve an appropriate workability [34]. The results of the average viscosity of all mixtures are presented in Table 5, along with the measured environmental temperature during the test and the workability of the mortars at the flow table. Viscosity was measured right after nine minutes of mixing.

Mixtures F, FS20, and FS30 did not give any results, because of their high viscosity. Due to the many factors involved in the test, more investigation is required in order to have more definite results. However, it could be said that higher percentages of concrete sludge reduce the viscosity of the mixtures. FA substitution with concrete sludge affects also the workability of the mixtures, by reducing water demand (Tables 3 and 4). High-calcium fly ash is known to have high water demand, mostly due to free calcium oxide content, and the use of concrete sludge seems to mitigate this effect, making it easier to achieve workable mortars.

Regarding strength development, Figure 5 shows the compressive strength test results for the mixtures without alkaline activation at 7, 28, and 90 days. In particular, the use of fly ash as binder showed relatively good strength results (16 MPa at 28 days) despite the high water to binder ratio.

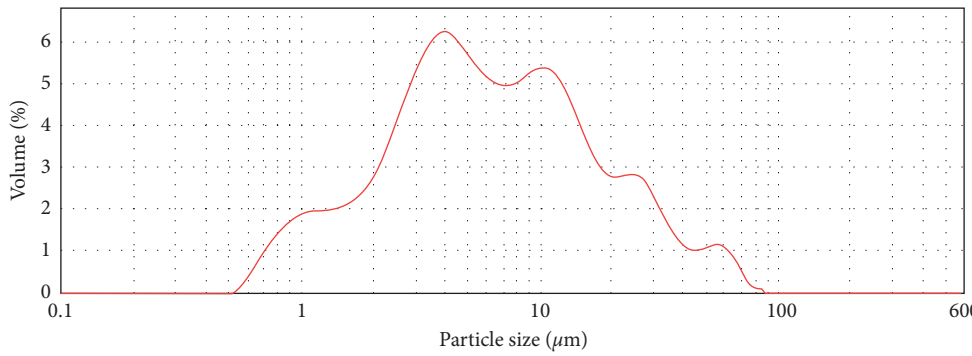

Figure 2: Particle size distribution of concrete sludge sieved under 75 μm (S75).

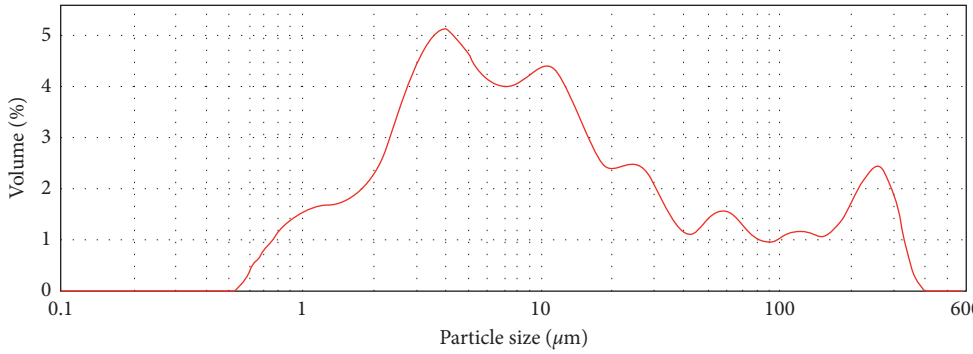

Figure 3: Particle size distribution of concrete sludge sieved under 200 μm (S200).

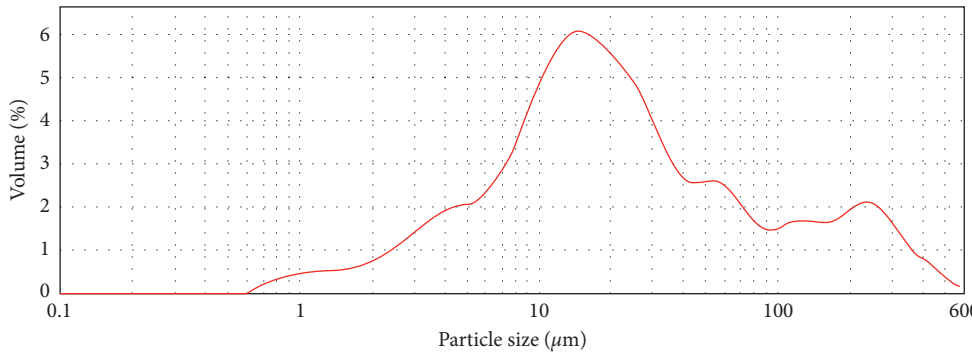

Figure 4: Particle size distribution of limestone filler (LF).

This could be attributed to the high contents of free calcium oxide and reactive silicon dioxide which are present in high-calcium fly ash. The reasonably low 7-day compressive strength of fly ash and the continued strength increase at 90 days indicate a slow rate of hydration mostly through the pozzolanic reaction. The replacement of up to 40% wt. of fly ash with concrete sludge inferred a slight 28-day compressive strength decrease (13–18%). Further increasing fly ash substitution rates to 50% and 60% resulted in considerably greater strength loss (29–43%). At earlier ages (7-day compressive strength), the differences from the various replacement rates were not very pronounced, while 90-day results showed improved results for lower replacement rates. A 22% strength increase was recorded for 20% substitution with concrete sludge, indicating an improvement in the hydration of fly ash. A smaller strength increase was observed for the 30% replacement rate, but overall increasing concrete sludge rate reduced strength proportionally.

Since the chemical composition of the concrete sludge used in these mortars (S75) was very similar to that of limestone filler (see Table 2), the improvement in the hydration of fly ash could be attributed to the filler effect. This effect is also observed when using limestone filler as cement substitution, which diminishes at higher substitution rates. However, mortar FF50 with 50% of fly ash substituted with limestone filler reached compressive strengths of 0.81 MPa at 7 days, 5.07 MPa at 28 days, and 7.92 at 90 days, a decrease of 85%, 56%, and 48% compared to mortar FS50 (50%

Table 1: Particle size distribution.

Sample	d10	d50	d90
F	3.51	29.68	191.09
S75	1.59	6.05	25.44
S200	1.82	8.35	143.82
LF	4.36	19.12	177.34

Table 2: Chemical composition (% wt) and pH values of raw materials.

Sample	Na_2O	K_2O	CaO	MgO	Fe_2O_3	Al_2O_3	SiO_2	SO_3	LOI	pH
F	0.92	1.14	22.58	1.87	5.08	17.85	46.83	3.68	2.92	13.75
S75	0.18	0.28	53.40	2.58	1.96	3.20	2.28	0.46	35.42	13.22
S200	0.18	0.09	39.95	1.56	1.18	3.55	15.01	0.50	38.17	11.87
LF	0.02	0.05	53.10	1.15	0.20	0.42	0.54	0.10	43.53	10.52

Table 3: Proportioning of test mortars.

Mixture	F (parts by mass)	CS75 (parts by mass)	LF (parts by mass)	Water/binder (parts by mass)	Natural river sand (parts by mass)	Superplasticizer (% by mass of the binder)
F	1.0	—	—	0.67	3.0	3.0
FS20	0.8	0.2	—	0.60	3.0	3.0
FS30	0.7	0.3	—	0.60	3.0	3.0
FS40	0.6	0.4	—	0.60	3.0	1.5
FS50	0.5	0.5	—	0.60	3.0	1.5
FS60	0.4	0.6	—	0.60	3.0	1.5
FF50	0.5	—	0.5	0.60	3.0	—

Table 4: Proportioning of alkali-activated mortars.

Mixture	F (parts by mass)	CS75 (parts by mass)	CS200 (parts by mass)	Liquid/binder (parts by mass)	Natural river sand (parts by mass)	Superplasticizer (% by mass of the binder)
AF	1.0	—	—	0.73	3.0	3.0
AFS20	0.8	0.2	—	0.67	3.0	3.0
AFS50	0.5	0.5	—	0.67	3.0	2.0
AN30/ AT30	0.7	—	0.3	0.67	3.0	3.0

substitution of fly ash with concrete sludge), respectively. These results indicate that concrete sludge has a different behavior than limestone filler and seems to contribute to the reaction mechanism. Another possible explanation for the higher reactivity of the mortars with concrete sludge is its high alkalinity (13.22 as opposed to 10.52 of limestone filler), which promotes hydration in the pore solution. The hydration products of the mortars with 50% fly ash replacement with either concrete sludge (FS50) or limestone filler (FF50) at 90 days were confirmed by the XRD diagrams and are presented in Figure 6.

The presence of inherent crystalline systems of calcite and quartz in all samples examined must be attributed mainly to the nature of the raw materials used (mixtures of fly ash with concrete sludge or limestone, at a ratio of 50 : 50). The phase of calcite is enhanced by the carbonation reaction of mixtures FS50 and FF50 during their exposure to atmospheric conditions for 90 days. The presence of gypsum and its anhydride is also observed in all mixtures, mainly due to the nature of the calcareous fly ash containing sulfates. The presence of crystalline phases of ettringite is due to the gradual hydration of sulfate phases of gypsum and anhydrite especially in the high alkaline environment (pH > 13) of the fly ash-concrete sludge mixture. In addition, the characteristic reflections of portlandite are identified and appear only in the diagram of FS50, as a product of long-term hydration possibly due to the nature of the concrete sludge [6]. Finally, secondary crystalline phases such as orthoclase and albite are detected, apparently due to the addition of siliceous sand.

In order to investigate further the hydration products of FS50 and FF50 mixtures at 90 days, DTA-TG analysis was applied and the thermographs presented in Figure 7 were obtained.

The peaks observed between 50°C and 200°C could be attributed to the presence of free water, as well as the bound water from the hydrated phases of calcium silicate hydrates, calcium aluminate hydrates, and sulphoaluminate hydrates [40–42]. Thus, the increase in the amount of nonevaporated water in FS50 mixture compared to FF50 mixture is probably due to an increase in the chemically bound water in C-S-H compounds in FS50 mixture [42]. The weight loss in

Table 5: Rheological properties of the mortars.

Mixture	Viscosity (Pa ∗ s)	Flow table workability (cm)	Laboratory temperature (°C)	Water/binder (parts by mass)
F	—	12.9	20.0	0.67
FS20	—	12.9	20.0	0.60
FS30	—	13.7	21.0	0.60
FS40	154.3	13.5	19.0	0.60
FS50	242.7	14.0	18.5	0.60
FS60	135.5	12.5	18.5	0.60
FF50	343.3	11.1	16.0	0.60

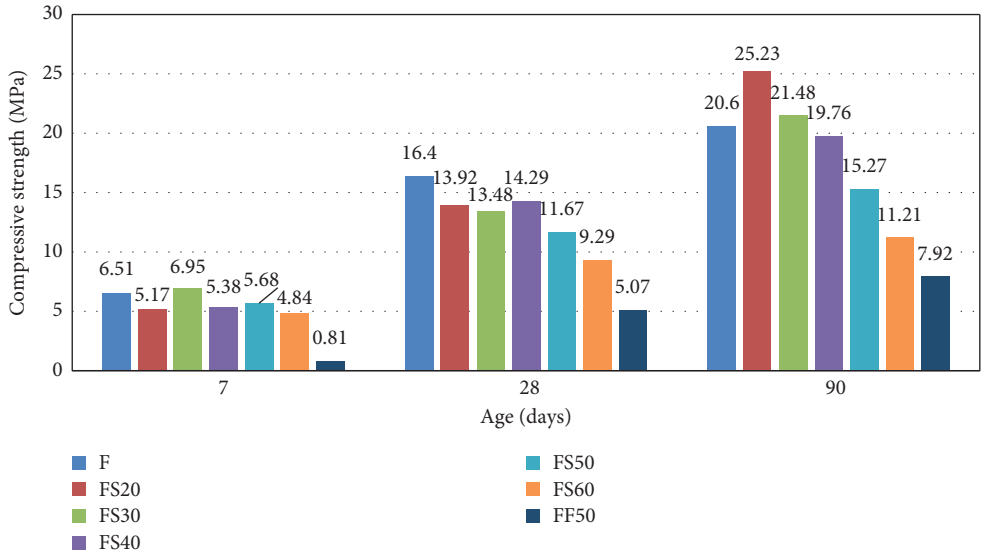

Figure 5: Compressive strength of nonactivated mortars at 7, 28, and 90 days.

the range of 400–450°C occurred mainly due to the dehydroxylation of calcium hydroxide, while the loss at 650–800°C was due to the decomposition of carbonates. The main difference between the two mortars is the loss of hydroxyls at 409–428°C for FS50 compared to FF50, interpreted as the presence of the hydration product $Ca(OH)_2$ of concrete sludge, probably increasing over time [2, 40–42].

The study of phase transformations of hydrated products at 90 days through the characteristic vibration bands and assignments (wavenumber in cm^{-1}) was conducted by taking spectra in the mid infrared by ATR technique and is presented in Figure 8 and Table 6.

The broad bands in the range of 3800–1600 cm^{-1} are generally assigned to vibration modes of bound water molecule and hydroxyls (HOH and –OH). The band at 3647 cm^{-1} observed in the hydrated product of the FS50 mixture is attributed to the hydroxyl anions of $Ca(OH)_2$. The band does not appear to the spectra of the FF50 mixture due to the nature of limestone. This agrees with the diagrams of XRD and TGA-DTA analyses, thus indicating the ability of FS50 components to give the hydration reaction possibly due to the cementitious nature of the sludge [2, 6]. The broad band at 3401 cm^{-1} in FS50 mixture was more intense compared to the FF50 mixture and this can be explained by the increased presence of hydrated products. The weak bands at 1626 cm^{-1} and at 1612 cm^{-1} in FS50 and FF50 mortars, respectively, are attributed to the bending deformation of HOH molecules. The bands at 1410 cm^{-1} and 874/711 cm^{-1} of the FS50 mortar and at 1407 cm^{-1} and 872/711 cm^{-1} of the FF50 mixture are attributed to $CaCO_3$ carbonates, which were mainly obtained from the carbonation process of the materials. The bands at 1103 cm^{-1} and 1144/1092 cm^{-1} in FS50 and FF50 mortars are attributed to the vibration of the sulphates group. Specifically, in the FS50 mortar, the band at 1103 cm^{-1} almost disappeared and was overlapped by the stretching vibration band of Si-O. The vibration strong band at 965 cm^{-1} of the FS50 mixture is worth noting, which increases in intensity and shifts to lower frequencies relative to the absorption of FF50 at 971 cm^{-1}, indicating the formation of amorphous C-S-H phase during the hydration process. Additionally, the changes observed in the region 670–450 cm^{-1} correspond to the bending vibrations from amorphous and crystalline aluminosilicates [43–47].

Porosity measurements at the age of 28 days, shown in Figure 9, confirm the compressive strength results of the mortars. When the amount of concrete sludge substitution was increased, compressive strength declined, and porosity increased accordingly. However, the measured values had a small variation overall, from 6.5% to 9.9%, and the use of

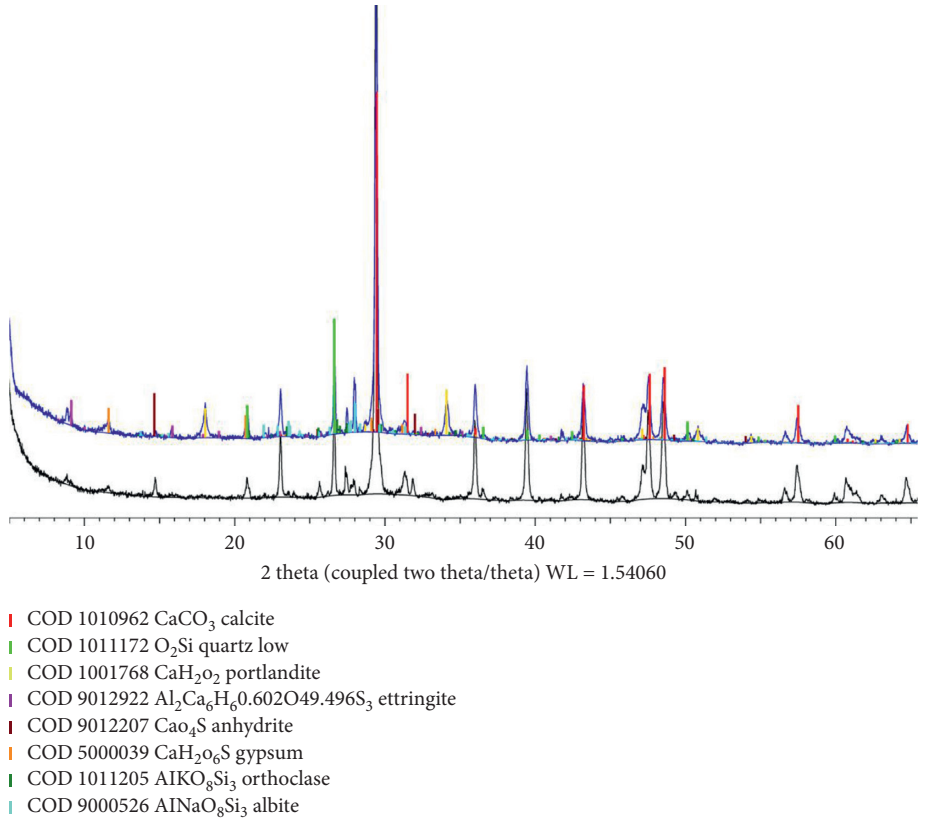

Figure 6: Diagrams of XRD analysis of mixtures FS50 (up) and FF50 (down) at 90 days.

concrete sludge did not alter mortar porosity considerably. Also, substitution of fly ash with limestone filler compared to concrete sludge did not change mortar porosity considerably either. Regarding early-age shrinkage measurements (Figure 10), the rate of volume shrinkage and percentile volume change was similar for all mortars and seems to stabilize at 25–30 days. This indicates that there were no significant early-age deformations arising from the combination of fly ash and concrete sludge; however, long-term shrinkage measurements should be made to establish adequate durability regarding deformation.

3.2. Alkali-Activated Mortars. The fresh properties of the selected mortar mixtures which were repeated with the addition of the alkaline activator are shown in Table 7. Compared to the nonactivated mortars (Table 5), the use of the activator seems to increase water demand regardless of the use of concrete sludge. However, the substitution of fly ash with concrete sludge still seems to improve the workability and viscosity of the mixtures, taking also into account the lower liquid/binder ratio. The coarser concrete sludge (S200) used in activated mortars AN30 and AT30 seemed to improve mostly viscosity rather than flow table workability, which could be attributed to its particle size distribution.

Figure 11 shows the values from the compressive strength tests of the alkali-activated mortars. Regarding the 100% high-calcium fly ash mortar, the addition of the alkaline activator enhanced compressive strength at early ages (15.29 MPa at 7 d) compared to the mixture with plain water (6.51 MPa at 7 d, Figure 5). This increase continued at the age of 28 days, where strength level of AF and F mixtures was around 19.99 MPa and 16.40 MPa, respectively. Again, the replacement of fly ash with concrete sludge (S75) at rates of 20% (AFS20) and 50% (AFS50) reduced the compressive strength up to 50%. However, the use of S200 concrete sludge had a great impact on the development of strength, since for mortar AN30, a 28-day compressive strength increase of 30% was observed. This is attributed to the chemical composition of S200 (Table 1), since S200 (<200 μm) had 15.01% content of silicon oxides, while S75 (<75 μm) had only 2.28% and the extra silicon oxide present is considered to contribute to this strength increase. When curing at 40°C for 24 hours was used to further enhance the alkali activation process (AT30), it was clear that it did not improve the mechanical characteristics of the mortar, as it appeared to reduce strength over 15% in all ages compared to AN30 (cured at 25°C). This has also been reported before by the authors, as it is proven that binders with a high lime content, such as fly ash and ladle furnace slag, do not require heating in order to develop high strength levels [34, 48]. However, the relative 28-day compressive strength increase for the alkali-activated mortars with

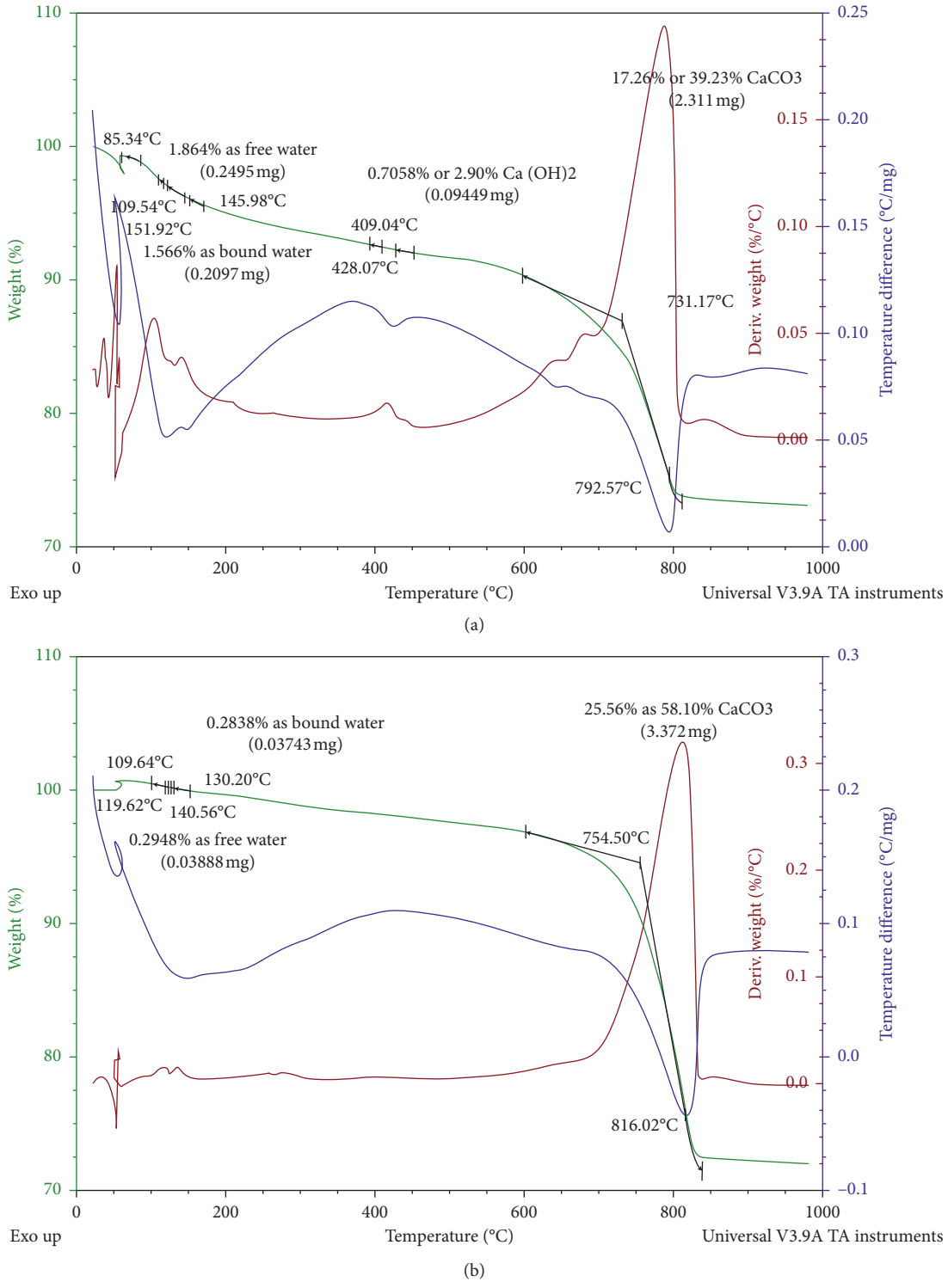

Figure 7: Thermographs of DTA-TG analysis of mixtures (a) FS50 and (b) FF at 90 days.

S200 was followed by a marked decrease at 90 days for both AN30 and AT30 mixtures, which shows limited gains by the activation process.

Porosity values of the alkali-activated mortars are presented in Figure 12 and the mortars with fly ash and S75 concrete sludge showed a reduction of around 30% compared to the same mixtures without alkali activation (Figure 9), which complies with the elevated compressive strength results. Alkali-activated mortars AN30 and AT30, however, showed considerably higher porosity values, despite the higher compressive strength results. This occurrence confirms the diverse performance of S75 and S200,

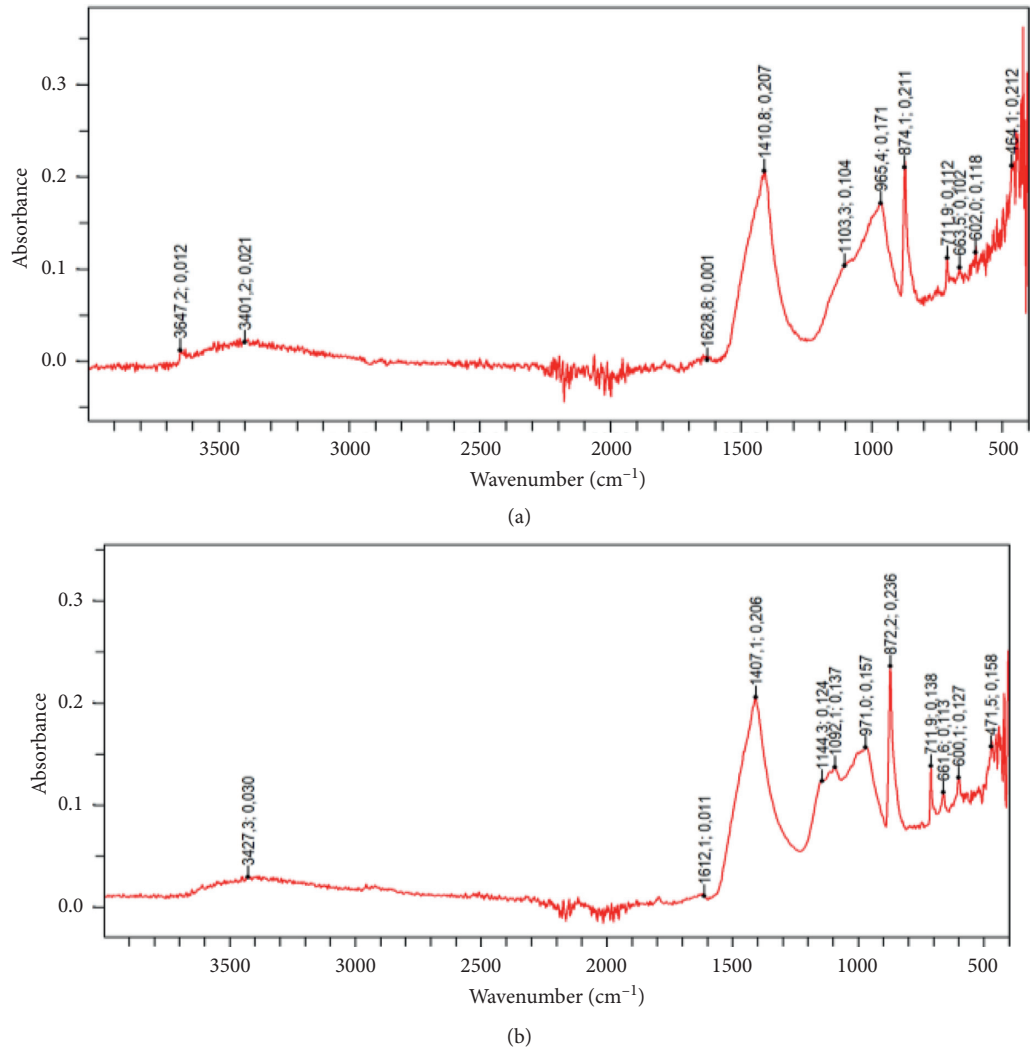

Figure 8: ATR-FTIR spectra analysis of mixtures (a) FS50 and (b) FF50 at 90 days.

Table 6: FTIR assignments (wavenumber in cm^{-1}) for the FS50 and FF50 mixtures at 90 days.

Assignments	FS50	FF50
Hydrogen bonds O-H ($Ca(OH)_2$) (stretching vibration)	3647	—
Hydrogen bonds O-H (H_2O) (stretching vibration)	3401	3427
HOH (bending vibration)	1626	1612
Carbonates, O-C-O (stretching vibration)	1410	1407
Sulphates, SO_4 = (anhydrite)	1103	1144/1092
Si-O (C-S-H) (stretching vibration)	965	971
Carbonates, O-C-O (stretching vibration)	874/711	872/711
Si-O-Si, Si-O-Si/Si-O-Al (bending vibration)	663, 602	661, 600
Si-O (SiO_4) (bending vibration)	464	471

owing to either different granulometry or different activity. The same pattern was observed regarding the early-age volume shrinkage test results (Figure 13). While the activated mortars with S75 showed a 28-day volume reduction of 5%–7%, higher than the nonactivated mortars (3.5–5%), the mortars with S200 had 28-day volume reduction limited to 2.5%. The volume reduction of all mortars gradually stabilized, while curing at 40°C (AT30) for 24 hours seem to affect the results neither of early-age shrinkage nor of porosity.

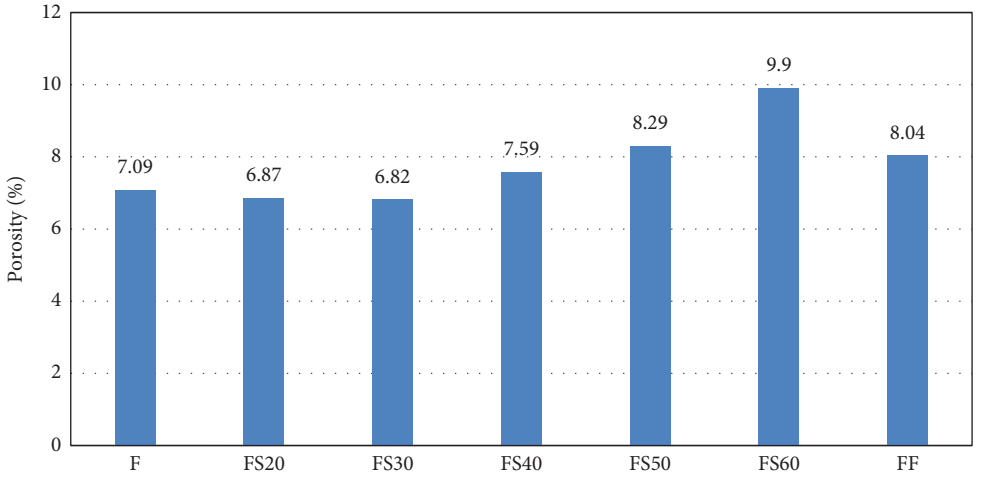

Figure 9: Porosity of the nonactivated mortars at 28 days.

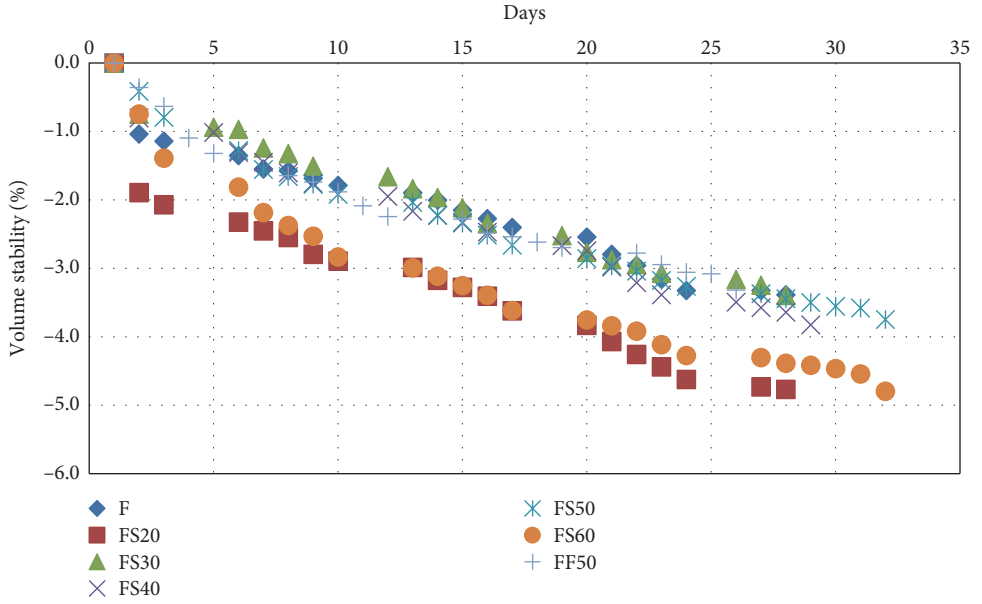

Figure 10: Volume stability of the nonactivated mortars.

Table 7: Rheological properties of alkali-activated mortars.

Mixture	Viscosity (Pa ∗ s)	Flow table workability (cm)	Laboratory temperature (°C)	Liquid/binder (parts by mass)
AF	385.2	11.8	16	0.73
AFS20	91.6	15.1	16	0.67
AFS50	63.1	16.1	16	0.67
AN30/AT30	29.5	12	15.5	0.67

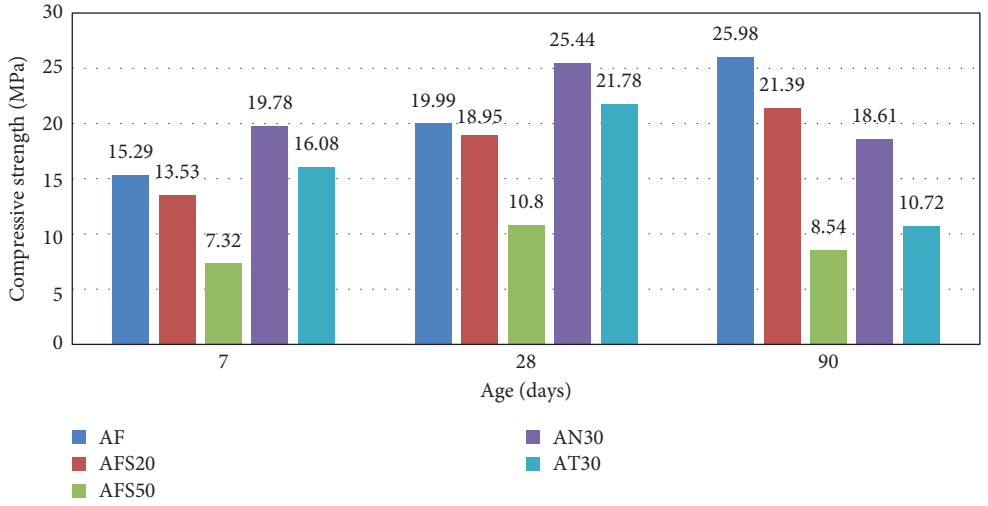

Figure 11: Compressive strength of alkali-activated mortars at 7, 28, and 90 days.

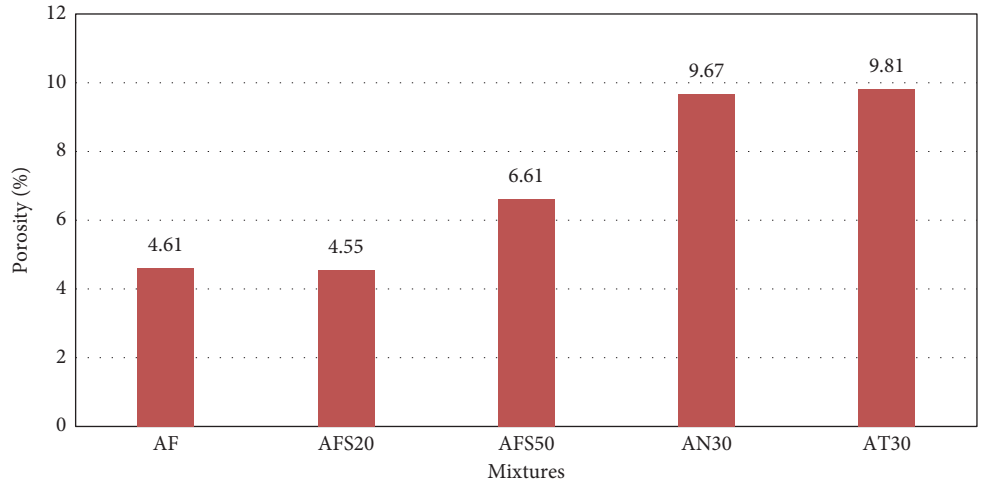

Figure 12: Porosity of alkali-activated mortars at 28 days.

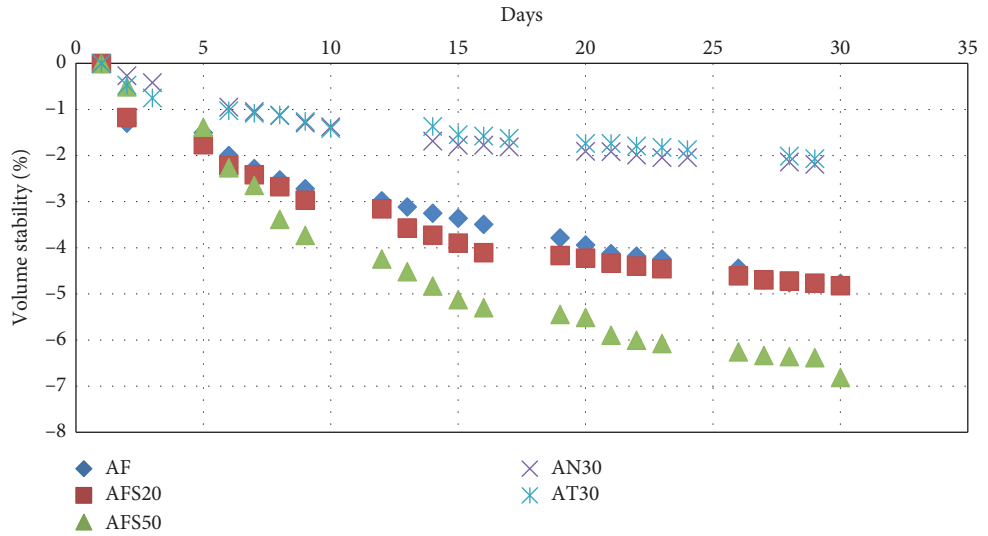

Figure 13: Volume stability of alkali-activated mixtures.

4. Conclusions

The present research investigated the potential combination of concrete sludge and high-calcium fly ash for mortar production.

(i) The high-calcium fly ash tested showed a slow but considerable strength development rate, reaching 16 MPa compressive strength at 28 days.

(ii) Fly ash substitution with concrete sludge had a positive effect on the rheology of mortars, since it reduced viscosity, improved workability, and reduced water demand.

(iii) Fly ash substitution rates of 20% and 30% showed the best results regarding strength development, starting with a slight reduction at 28 days and eventually improving strength at 90 days. Higher replacement rates, however, showed a decrease in strength development, proportional to the concrete sludge used.

(iv) Analytical tests in comparison with fly ash-limestone filler mortars confirmed that concrete sludge promotes the hydration of fly ash and the formation of C-S-H. XRD analysis confirmed the presence of crystalline phases of ettringite and the characteristic reflections of portlandite in the mortar with 50% concrete sludge. According to the DTA-TG analysis, the main difference between the fly ash-concrete sludge and the fly ash-limestone filler mortars was the loss of hydroxyls at 409–428°C, as a presence of hydration product $Ca(OH)_2$ of concrete sludge which probably increases with time. The cementitious nature of the sludge is also certified through the ATR-FTIR spectra analysis. Porosity and early-age shrinkage did not alter significantly when concrete sludge was used in the mortars.

(v) The alkali-activation mechanism increases water demand of the mortars, but the inclusion of concrete sludge still improves its rheological properties and decreases plastic viscosity of high-calcium fly ash-based mortars.

(vi) Regarding the mechanical properties, an improvement of earlier-age (7 and 28 days) compressive strength was observed with the addition of the alkaline activator in all cases. The same as in nonactivated mortars, increasing rates of concrete sludge replacement resulted in proportionally lower compressive strengths.

(vii) Thermal curing of the alkali-activated mortar at 40°C did not seem to promote compressive strength development, but rather decreased strength.

(viii) The chemical composition of the concrete sludge played an important role to the mechanism. This difference in chemical composition was obtained through sieving of the material under 75 μm or under 200 μm and thus obtaining a finer fraction of concrete sludge with low silicon oxide content (S75) and a coarser fraction with higher silicon oxide content (S200).

(ix) The mortars with 30% fly ash replacement with S200 sludge developed higher 28-day compressive strength, but strength decreased at 90-days.

(x) Overall, the alkali-activated mortars using the coarser concrete sludge with higher silicon oxide content had higher porosity and reduced early-age shrinkage S200, but further investigation is required regarding the alkali activation of concrete sludge.

(xi) After further research, especially regarding long-term properties and durability, these mortars could be used as masonry mortars and in low strength applications such as renders, paving slabs, and blocks. Studies regarding the environmental footprint of the mortars with fly ash and concrete sludge, such as comparative life cycle assessment, would highlight their environmental benefits.

Data Availability

The underlying data supporting the results of our study are available by the authors upon request.

Conflicts of Interest

The authors declare that they have no conflicts of interest.

References

[1] D. Xuan, B. Zhan, C. S. Poon, and W. Zheng, "Innovative reuse of concrete slurry waste from ready-mixed concrete plants in construction products," *Journal of Hazardous Materials*, vol. 312, pp. 65–72, 2016.

[2] M. Audo, P.-Y. Mahieux, and P. Turcry, "Utilization of sludge from ready-mixed concrete plants as a substitute for limestone fillers," *Construction and Building Materials*, vol. 112, pp. 790–799, 2016.

[3] B. J. Sealey, P. S. Phillips, and G. J. Hill, "Waste management issues for the UK ready-mixed concrete industry," *Resources, Conservation and Recycling*, vol. 32, no. 3-4, pp. 321–331, 2001.

[4] J. A. Férriz Papí, "Recycling of fresh concrete exceeding and wash water in concrete mixing plants," *Materiales de Construcción*, vol. 64, no. 313, p. e004, 2014.

[5] M. Paolini and R. Khurana, "Admixtures for recycling of waste concrete," *Cement and Concrete Composites*, vol. 20, no. 2-3, pp. 221–229, 1998.

[6] Y. Xi, E. Anastasiou, A. Karozou, and S. Silvestri, "Fresh and hardened properties of cement mortars using marble sludge fines and cement sludge fines," *Construction and Building Materials*, vol. 220, pp. 142–148, 2019.

[7] V. M. Malhotra, "High-performance high-volume fly ash concrete," *Concrete International*, vol. 24, no. 7, pp. 30–34, 2002.

[8] I. Papayianni and E. Anastasiou, "Production of high-strength concrete using high volume of industrial by-products," *Construction and Building Materials*, vol. 24, no. 8, pp. 1412–1417, 2010.

[9] F. Faleschini, M. A. Zanini, K. Brunelli, and C. Pellegrino, "Valorization of co-combustion fly ash in concrete production," *Materials & Design*, vol. 85, pp. 687–694, 2015.

[10] European Committee, *EN 450-1: 2012. Fly Ash for Concrete. Definition, Specifications and Conformity Criteria*, European Committee, Brussels, Belgium, 2012.

[11] Q. Zhou, C. Lu, W. Wang, S. Wei, C. Lu, and M. Hao, "Effect of fly ash and sustained uniaxial compressive loading on chloride diffusion in concrete," *Journal of Building Engineering*, vol. 31, Article ID 101394, 2020.

[12] E. K. Anastasiou, A. Liapis, and I. Papayianni, "Comparative life cycle assessment of concrete road pavements using industrial by-products as alternative materials," *Resources, Conservation and Recycling*, vol. 101, pp. 1–8, 2015.

[13] I. Papayianni and E. K. Anastasiou, "An investigation of the behavior of raw calcareous fly ash in mortar mixtures," *CCGP Journal*, vol. 2, no. 1, 2010.

[14] European Committee, *EN 197-1:2011. Cement—Part 1: Composition, Specifications and Conformity Criteria for Common Cements*, European Committee, Brussels, Belgium, 2011.

[15] European Committee, *EN 196-1:1995. Methods of Testing Cement—Part 1: Determination of Strength*, European Committee, Brussels, Belgium, 1995.

[16] I. Papayianni, S. Konopisi, K. Datsiou, and F. Kesikidou, "Products of alkali-activated calcareous fly ash and glass cullet," *International Journal of Research in Engineering and Technology*, vol. 3, no. 25, pp. 43–51, 2014.

[17] C. Shi, P. Krivenko, and D. Roy, *Alkali-activated Cements and Concrete*, Taylor & Francis, Abingdon-on-Thames, UK, 2006.

[18] J. L. Provis and J. S. J. van Deventer, "Alkali-activated materials," *State of the Art Report, RILEM TC 224-AAM*, Vol. 13, Springer, Berlin, Germany, 2014.

[19] S. Alonso and A. Palomo, "Alkaline activation of metakaolin and calcium hydroxide mixtures: influence of temperature, activator concentration and solids ratio," *Materials Letters*, vol. 47, no. 1-2, pp. 55–62, 2001.

[20] D. Bondar, C. J. Lynsdale, N. B. Milestone, N. Hassani, and A. A. Ramezanianpour, "Effect of type, form, and dosage of activators on strength of alkali-activated natural pozzolans," *Cement and Concrete Composites*, vol. 33, no. 2, pp. 251–260, 2011.

[21] X. Ke, S. A. Bernal, N. Ye, J. L. Provis, and J. Yang, "One-part geopolymers based on thermally treated red mud/NaOH blends," *Journal of the American Ceramic Society*, vol. 98, no. 1, pp. 5–11, 2015.

[22] M. Palacios, M. M. Alonso, C. Varga, and F. Puertas, "Influence of the alkaline solution and temperature on the rheology and reactivity of alkali-activated fly ash pastes," *Cement and Concrete Composites*, vol. 95, pp. 277–284, 2019.

[23] A. Fernández-Jiménez and A. Palomo, "Composition and microstructure of alkali activated fly ash binder: effect of the activator," *Cement and Concrete Research*, vol. 35, no. 10, pp. 1984–1992, 2005.

[24] D. W. Law, A. A. Adam, T. K. Molyneaux, I. Patnaikuni, and A. Wardhono, "Long term durability properties of class F fly ash geopolymer concrete," *Materials and Structures*, vol. 48, no. 3, pp. 721–731, 2015.

[25] C. D. Atiş, E. B. Görür, O. Karahan, C. Bilim, S. Ilkentapar, and E. Luga, "Very high strength (120 MPa) class F fly ash geopolymer mortar activated at different NaOH amount, heat curing temperature and heat curing duration," *Construction and Building Materials*, vol. 96, pp. 673–678, 2015.

[26] P. Chindaprasirt, T. Chareerat, and V. Sirivivatnanon, "Workability and strength of coarse high calcium fly ash geopolymer," *Cement and Concrete Composites*, vol. 29, no. 3, pp. 224–229, 2007.

[27] X. Guo, H. Shi, and W. A. Dick, "Compressive strength and microstructural characteristics of class C fly ash geopolymer," *Cement and Concrete Composites*, vol. 32, no. 2, pp. 142–147, 2010.

[28] A. Fernandez-Jimenez, I. García-Lodeiro, and A. Palomo, "Durability of alkali-activated fly ash cementitious materials," *Journal of Materials Science*, vol. 42, no. 9, pp. 3055–3065, 2007.

[29] D. Xuan, C. S. Poon, and W. Zheng, "Management and sustainable utilization of processing wastes from ready-mixed concrete plants in construction: a review," *Resources, Conservation and Recycling*, vol. 136, pp. 238–247, 2018.

[30] M. U. Hossain, D. Xuan, and C. S. Poon, "Sustainable management and utilisation of concrete slurry waste: a case study in Hong Kong," *Waste Management*, vol. 61, pp. 397–404, 2017.

[31] M. Zervaki, C. Leptokaridis, and S. Tsimas, "Reuse of by-products from ready-mixed concrete plants for the production of cement mortars," *Journal of Sustainable Development of Energy, Water and Environment Systems*, vol. 1, no. 2, pp. 152–162, 2013.

[32] I. Mehdipour, A. Kumar, and K. H. Khayat, "Rheology, hydration, and strength evolution of interground limestone cement containing PCE dispersant and high volume supplementary cementitious materials," *Materials & Design*, vol. 127, pp. 54–66, 2017.

[33] European Committee, *EN 451-1:1995.Method of testing fly ash—Part 1: Determination of free calcium oxide content*, European Committee, Brussels, Belgium, 1995.

[34] I. Papayianni, S. Konopisi, and F. Kesikidou, "Physico-mechanical properties and durability aspects of alkali-activated calcareous fly ash/slag mortars," *Key Engineering Materials*, vol. 761, pp. 87–91, 2018.

[35] European Committee, *EN 1015-3:2003, Methods of Test for Mortar for Masonry—Part 3: Determination of Consistence of Fresh Mortar*, European Committee, Brussels, Belgium, 2003.

[36] European Committee, *EN 1015-11:2006 Methods of Test for Mortar for Masonry—Part 11: Determination of Flexural and Compressive Strength of Hardened Mortar*, European Committee, Brussels, Belgium, 2006.

[37] RILEM TC, "CPC 11.3 absorption of water by concrete by immersion under vacuum," *RILEM Recommendations for the Testing and Use of Constructions Material*, pp. 36-37, RILEM, Paris, France, 1984.

[38] P. C. Aïtcin and R. J. Flatt, *Science and Technology of Concrete Admixtures, Series in Civil and Structural Engineering*, Woodhead Publishing, Cambridge, UK, 59th edition, 2016.

[39] M. M. Alonso, S. Gismera, M. T. Blanco, M. Lanzón, and F. Puertas, "Alkali-activated mortars: workability and rheological behaviour," *Construction and Building Materials*, vol. 145, pp. 576–587, 2017.

[40] G. Liptay, *Atlas of Thermoanalytical Curves: (TG-, DTG-, DTA-Curves Measured Simultaneously)*, Heyden and Son, Hoboken, NJ, USA, 1971.

[41] F. Deschner, F. Winnefeld, B. Lothenbach et al., "Hydration of Portland cement with high replacement by siliceous fly ash," *Cement and Concrete Research*, vol. 42, no. 10, pp. 1389–1400, 2012.

[42] P. Hewllet, *Lea's Chemistry of Cement and Concrete*, Elsevier Science & Technology Books, London, UK, 4th edition, 2004.

[43] H. F. W. Taylor, *Cement Chemistry*, Academic Press, Cambridge, MA, USA, 1990.
[44] V. C. Farmer, *The Infrared Spectra of Minerals*, Mineralogical Society, London, UK, 1974.
[45] W. Mozgawa, M. Sitarz, and M. Rokita, "Spectroscopic studies of different aluminosilicate structures," *Journal of Molecular Structure*, vol. 511-512, pp. 251–257, 1999.
[46] Y. Ping, R. J. Kirkpatrick, B. Poe, P. F. McMillan, and X. Cong, "Structure of calcium silicate hydrate (C-S-H): near-, mid-, and far-infrared sprectoscopy," *Journal of the American Ceramic Society*, vol. 82, no. 3, pp. 742–748, 2004.
[47] I. García Lodeiro, A. Fernández-Jimenez, A. Palomo, and D. E. Macphee, "Effect on fresh C-S-H gels of the simultaneous addition of alkali and aluminium," *Cement and Concrete Research*, vol. 40, no. 1, pp. 27–32, 2010.
[48] I. Papayianni, S. Konopisi, and F. Kesikidou, "Alkali activation of ladle furnace slag (LFS). effect of fineness, curing regime and concentration of activator on mechanical and physical characteristics of LFS pastes," in *Proceedings of the 10th European Slag Conference*, Thessaloniki, Greece, October 2019.